

Spatiotemporal Waveform Observers and Feedback in Shear Layer Control

Mark Pastoor*, Bernd R. Noack[†] and Rudibert King[‡]

Sfb 557, Technical University of Berlin, Straße des 17. Juni, 10623 Berlin, Germany

Gilead Tadmor[§]

Communication & Digital Signal Processing Center,

Northeastern University, 440 Dana Research Building, Boston, MA 02115, U.S.A.

Active control enhances shear layer mixing by exciting natural instabilities. Harmonizing the periodic actuation with vortex release can be used to manipulate and improve the mixing effect. This type of feedback requires tracking large shear layer vortices. We propose an observer structure based on a very simple model, representing the collective signal of a set of sensors as a spatiotemporal waveform. The observer tracks the slow drift and abrupt changes in the spatiotemporal phasors (local Fourier coefficients). Benefiting from a much longer time constant than the period of vortex release, it naturally filters spatial and temporal high frequency noise. The discussion is illustrated by simulations and wind tunnel experiments for the flow over a backward facing step, where the design objective is shortening the recirculation bubble. Simulations of the free shear layer are used to illustrate means to track asynchronous vortex merging events.

I. Introduction

Shear layer flows are unstable and sensitive to periodic perturbations,¹⁻³ a phenomenon known as *Kelvin-Helmholtz* instability. The instability is manifest by the periodic release of vortices that convect and grow along the shear layer, undergo a series of pairwise merging into larger and larger structures, and eventually dissipate into the flow. Mixing enhancement in shear layers is a standard objective, associated, e.g., with pressure recovery in aggressive diffusers⁴ and flame stabilization in a turbine engine combustor.⁵

Pulsating synthetic jet actuation, exciting selected vortex release frequencies, has been established as an effective tool to either enhance or suppress shear layer instabilities. In particular, periodic excitation at the natural resonance frequency is an effective means to enhance mixing⁶ and it tends to reduce aperiodic modulations, typical of the natural flow. This harmonization effects is desirous in its own right, under a mixing objective, as it reduces the attenuating effect of out-of-phase waveforms. Feedback is sought as a means to both improve and, when desired, to regulate shear layer growth and mixing, by enhancing growth at the resonance frequency.

Considering the ubiquitous backward facing step benchmark, early shear layer oscillations are hard to discern, but vortex release can be inferred from the position of downstream vortical structures. In the presence of sinusoidal synthetic jet actuation, simulations analysis reveals that, on average, vortex release coincides with peak blowing, in agreement with an intuitive perception of the effect of the actuation. This further suggests that shear layer growth can be regulated by controlling the phase difference between actuation and vortex release: Instantaneous phase differences are both well expected, due to disturbances, unmodeled low

*Doctoral Student

[†]Ass. Professor

[‡]Professor and Sfb 557 Director

[§]Professor, CDSP Director

Copyright © 2006 by M. Pastoor, B.R. Noack, R. King & G. Tadmor. Published by the American Institute of Aeronautics and Astronautics, Inc. with permission.

frequency dynamics and the like, and are indeed observed in both simulations and experiments. If the suggested intuition is correct, phase mismatch between actuation and shear layer dynamics has an attenuating effect, due to the coexistence of out-of-phase harmonics in the flow. Feedback regulation that suppresses perturbation from the ideal regimentation of actuation and shear layer dynamics is therefore expected to remove these attenuating effects and enhance shear layer growth. Likewise, feedback imposition of a different phase is expected to lower the growth rate. This note develops and tests the tools to demonstrate this hypothesis.

A key component of the sought feedback algorithm is the ability to dynamically reconstruct the position and motion of shear layer vortices. This issue is viewed here as part of the wider and relatively recent undertaking of developing new model based feedback control methods, specifically for fluid flow systems (see e.g. the books & reviews^{7–11} and our own work^{5, 12–16} and relating modeling results^{17, 23}). A major component of this effort is the development of models suitable for design, addressing real time implementation issues such as complexity sensitivity and nonlinearity system. Common examples include very low order vortex models^{5, 18–22} and very low order Galerkin models.^{14–17, 23}

Here we focus on a yet simpler modeling framework, exploiting the flip side of a generic restriction of feasible control to slow manipulation of phase in nearly periodic actuators, such as the pulsating synthetic jet. In that context we propose a modeling framework that is focused on the representation of sensor signals in terms of traveling waveforms with slowly varying Fourier coefficients (also known as *dynamic phasors*^{24, 25}), which are the subject of dynamic estimation. Following our preliminary results in,^{13, 26} this article examines the development of such models and their application to feedback, in the backward facing step benchmark, as well as in the ideal two dimensional free shear layer, where an added complexity is introduced by asynchronous vortex merging.

II. Observation and Control of the Backward Facing Step

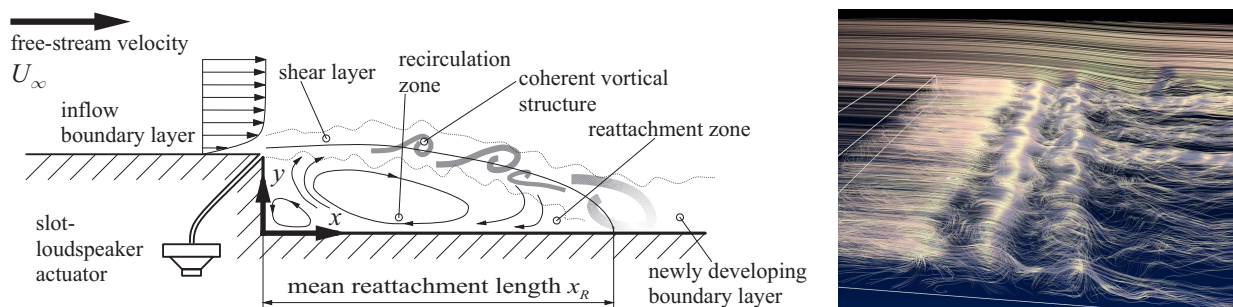


Figure 1. Flow field downstream of a backward-facing step. **Left:** A schematic of our experimental testbed. **Right:** A detailed 3D Large Eddy simulation from Ref.²⁷

A. The flow over a backward facing step

The discussion in this section is based on an experimental setup which is schematically sketched in Fig. 1. The flow detaches at the step and reattaches downstream. The wake area of current interest comprises a recirculation bubble bounded by a shear layer and a reattachment zone. Sinusoidal zero net flow actuation through a slot at the corner is effected by a loudspeaker, allowing for slow modulation of actuation amplitude and phase. In the context of this note, actuation is used to excite faster shear layer growth to enhance mixing. Reattachment in the natural flow is at over six step-heights downstream, whereas the increased stirring motion under open loop actuation at or near the natural instability frequency can bring it to about four step-heights. The actuation frequency and amplitude will be denoted ω and A , respectively:

$$a(t) = A \sin(\phi_a), \quad \frac{d}{dt} \phi_a = \omega \quad (1)$$

The reattachment point is determined in terms of the (period) average location of the zero shear stress point on the wall. Kelvin-Helmholtz vortices evolve along the shear layer and become large enough to be apparent at about two step-heights downstream. At Reynolds number of 4000 (calibrated with respect to step height), the shear layer above the recirculation and the reattachment zones typically comprises 2–4 vortical structures (depending on the actuation frequency), where the downstream pair merges to form a

larger structure. While dynamically much simpler than the free shear layer, modeling the backward facing step benchmark includes challenging asynchronous perturbations due to low frequency modulation of vortex release and merging.

Previous studies of feedback control of this system at TU Berlin aimed to regulate the reattachment point, using the actuation voltage amplitude as a command signal. Flow information is obtained from an array of 15 pressure gages (microphones) on the floor of the reattachment zone, using the finding, that the maximum of the pressure fluctuations is at 90% of the reattachment length.²⁸⁻³⁰

Here the objective is to refine the control command with flow phase actuation: Simulations of the sinusoidally actuated flow reveal that the average actuation phase is $\phi_a = 0.5\pi \text{ mod } 2\pi$ at the release of a new vortex. Since the flow responds to a destabilizing perturbation by synchronizing its unstable mode with the actuation, this phase coincidence is viewed as optimal for shear growth, and the design objective set forth is to introduce slow corrections into the actuation, to compensate for occasional spontaneous and disturbance driven drifts from this phase relation^a. That is, control design, in this note, concerns slow feedback corrections to the phase dynamics, in (1).

The flow phase is defined by the (nearly) periodic vortex release at the step corner. A dynamic observer, estimating the flow phase, is a critical component in this scheme. As mentioned above an array of microphones is aligned in the stream-wise direction, on the step floor. The microphones provide readings $\mathbf{p}_i(t)$ of the short time pressure fluctuations $\mathbf{p}'_w(t, \mathbf{x})$ (where $\mathbf{x} = (x, y)$ is the location of a point in the 2D section in which the microphones are located). Pressure fluctuations at each point result from the low pressure associated with passing shear layer vortices. Thus, the traveling wave formed by $\mathbf{p}'_w(t, \mathbf{x})$ has a fixed nominal phase relations to shear layer vortices flow and the control objective can be restated in terms of a desired relation between the actuation phase and the phase of that traveling wave, as determined from long term average of the sinusoidally actuated flow. Experiments validate the theoretically predicted 0.5π phase difference between the vortex wave form and the measured pressure waveform, and the optimal design objective is thus to keep the actuation *in phase* with the waveform $\mathbf{p}'_w(t, \mathbf{x})$.

B. Observer Design and Feedback

One approach to locate shear layer vortices is to solve an instantaneous inverse problem, directly from a detailed flow model (e.g., a Lagrangian vortex model)^{31,32}. This approach suffers from several potential disadvantages, including the required number of sensors, and numerical ill-conditioning, and noise effect. Whether explicitly or implicitly, the common practice in feedback engineering is to exploit a priori assumption concerning the dynamics of a system, to alleviate these difficulties. Indeed, the use of dynamic observers has the dual effect of adding time trajectory data to the solution of inverse problem at each point in time, and of filtering unmodeled noise. Here we consider a very simple modeling option, which was previously tested in the context of a rotating vortex pair:¹³ The temporally and spatially periodic traveling waveform $\mathbf{p}'_w(t, \mathbf{x})$ is ideally represented by a fixed set of Fourier coefficients, or *phasors*. The system model is then reduced to a slow drift in these phasors, driven by a disturbance. Extracting the *innovation signal* from a comparison of sensor readings projection on the waveforms subspace and the predicted waveform is an effective means for filtering pervasive high frequency perturbations and random span-wise dynamics in the flow (i.e., in the orthogonal direction to the crosscut plane of Figure 1).

The detection of vortex release in terms of the position of downstream vortices creates a delay of roughly one convection time period in the feedback loop. As in any other control system, this delay restricts feasible closed loop bandwidth to time constants that are significantly longer than that delay. Additionally, high bandwidth and high gain actuation can introduce flow structures that deviate significantly from the postulated periodically dominated flow, or for that matter, the predictive power of any very low order model. Control and observer parameters are thus selected to adhere to the rather limited dynamic repertoire that such a model can cover. Following are specific steps in the suggested algorithm. Preprocessing of raw sensor data comprise of the following:

- Microphones capture pressure fluctuations and induce frequency dependent nonlinear phase shift and damping. These effects are calibrated against ideal values of $\mathbf{p}'_w(t, \mathbf{x}_i)$, where \mathbf{x}_i is the i^{th} microphone location.

^aWe are content here with a heuristic justification of the chosen design objective, for two reasons: To begin with, it serves the essence of this benchmark study, which is rather to demonstrate the utility of dynamic phasor estimation for phase corrections in nearly periodic flow and actuation, as detailed below. Moreover, while a rigorously found objective could be based, say, on adjoint optimization of a well defined cost function, our criterion is well grounded in basic tenets of fluid mechanics, and its validity in the current context will be demonstrated in experimental results.

- In addition to the effect of passing shear layer vortices, pressure fluctuations are caused by external acoustic disturbances and are subject to drift. Both the effect of remote sources and slow drift are characterized by relatively low spatial frequency, hence similar impact on the (calibrated) readings of all sensors. That component is removed by subtracting the calibrated value of one sensor reading from those of all the other sensors.
- Due to vortex growth and shear-layer bending, pressure fluctuations increase in the downstream direction. The envelope varies as a function of changes in the reattachment point, and is determined by a combination of an off-line, long term computation in a preprocessing step, and low-pass real time correction. Sensor readings are normalized by the envelope amplitude, to create readings of an ideal sinusoidal traveling wave. The normalized instantaneous value of the i^{th} sensor are denoted \mathbf{p}_i^n .

The normalized traveling waveform representation of the sensor readings is ideally of the form

$$\begin{aligned}\mathbf{p}_i^n(t) &= R \sin(\phi_w(t) - 2\pi x_i/\lambda) \\ &= R \sin(\phi_a(t) + \phi_d - 2\pi x_i/\lambda)\end{aligned}\quad (2)$$

where $\phi_w(t)$ is defined as the phase of the pressure fluctuation wave form, $\phi_a(t)$ is the actuation phase, as in (1), λ is the spatial period and ϕ_d stands for the *phase difference* between the normalized traveling wave and the actuation. In particular, the nominal natural dynamics are determined by (1) and a postulated constant wave length λ .

$$\frac{d}{dt}\phi_w = \omega, \quad \frac{d}{dt}\lambda = 0 \quad (3)$$

The instantaneous spatial Fourier coefficients of the combined sensor readings are

$$\begin{aligned}\alpha(t) &= R \sin(\phi_w(t)) = R \cos(\phi_a(t) + \phi_d) \\ \beta(t) &= R \cos(\phi_w(t)) = R \sin(\phi_a(t) + \phi_d)\end{aligned}\quad (4)$$

and our control objective is stated in terms of a target value ϕ_{d*} for ϕ_d , whether ϕ_{d*} is assigned the ideal value of $\phi_{d*} = 0$ or otherwise.

The need for feedback is due to the possibility (indeed, likelihood) for slow drift in both R , λ and ϕ_d . For example, fluctuations in λ (and R) will result from changes in the mean incoming flow velocity. Other causes include low frequency dynamics in both the span-wise and stream wise directions that are not manifest in low order models. The next processing steps aim to extract measurements of R , λ and ϕ_d from sensor data:

- The instantaneous measurements $\mathbf{p}_i^n(t)$ are projected (using straightforward least mean square approximation) on the spatial harmonic modes $\cos(\frac{2\pi}{\lambda_j}x)$ and $\sin(\frac{2\pi}{\lambda_j}x)$, for an array of wave lengths λ_j , to obtain associated first harmonic spatial Fourier coefficient pairs $(\alpha_j(t), \beta_j(t))$. Using the subscript “ m ” to indicate the value selected as the measured quantity, the instantaneous measured wave length λ_m and the associated measured $(\alpha_j(t), \beta_j(t))$ are those for which the *measured* amplitude $R_m = \sqrt{\alpha_m^2 + \beta_m^2}$ is the largest among $R_j = \sqrt{\alpha_j^2 + \beta_j^2}$. The *measured* oscillation phase is $\phi_m(t) = \angle(\alpha_m(t), \beta_m(t))$.
- Dynamic observers, estimating the values of λ and ϕ , are simple 1^{st} order low pass filters, suppressing high frequency disturbances. Implemented in discrete time these are of the form

$$\begin{aligned}\widehat{\lambda}(t_{k+1}) &= (1 - \sigma)\widehat{\lambda}(t_k) + \sigma\lambda_m(t_{k+1}) \\ \widehat{\phi}_w(t_{k+1}) &= (1 - \rho)(\widehat{\phi}_w(t_k) + \Delta t\omega) + \rho\phi_m(t_{k+1})\end{aligned}\quad (5)$$

where $0 < \sigma, \rho \ll 1$ are the filter coefficients and $\Delta t = t_{k+1} - t_k$ is the time step.

An estimate $\widehat{\mathbf{p}}_w'(t, \mathbf{x})$ of the distributed pressure fluctuations can now be obtained by reversing the normalization step, using R_m (or a low pass filtered version) and the estimated $\widehat{\lambda}$ and $\widehat{\phi}_w$ in (2). That estimate, however, is unnecessary. The practical aspect of the estimation is the correction for drift in ϕ_d in the actuation:

- The actuation phase at the time t_k is determined by the estimated phase of the sensor signal wave form and the designated ϕ_{d*} .

$$\phi_a(t_k) = \widehat{\phi}_w(t_k) - \phi_{d*} \quad (6)$$

C. Experimental Results

The algorithm was implemented in the testbed in Figure 1. The step height is $H = 2\text{cm}$ and the incoming flow velocity is $U_0 \approx 3\text{m/s}$, corresponding to a Reynolds number of 4000. The actuation frequency of 30Hz corresponds to a Strouhal number of $St \approx 0.2$, meaning an actuation period of $T_a \approx 5$ convection time units. The actuation voltage amplitude is set at $A = 200\text{mV}$. The controller clock is set at 1kHz , meaning that $\Delta t = 0.15$ convection time units. The spatial wave length filter was designed with a convergence time constant of $10T_a$ and the filter for the estimated pressure waveform phase, with a time constant of in a range from $0.05T_a$ to $1.0T_a$. This means that we use $\sigma = \Delta t/10T_a$ and $\rho = \Delta t/0.05T_a$ to $\rho = \Delta t/T_a$.

Results are depicted in Figure 2. The left plot displays the maximum of pressure fluctuations (rms-values) for the natural flow, and for the flow under open- and closed-loop actuation. Phase estimation occurred with $\rho = \Delta t/0.5T_a$. Feedback actuation yields higher fluctuation levels as open-loop, with a minimum at $\phi_{d^*} = 0$ and increasing levels for higher and lower commanded ϕ_{d^*} . However, the right plot reveals, that the reattachment length x_R , and therefor the location of the pressure maximum, is shifted compared to open-loop actuation. Commanding $\phi_{d^*} > 0$ apparently hampers mixing and increases the reattachment length, while $\phi_{d^*} < 0$ enhances mixing and thus decreases the length of the recirculation bubble. The tracking capability of the observer deteriorates at very high and very low ϕ_{d^*} , respectively. This puts a limit to both increase and decrease of efficiency.

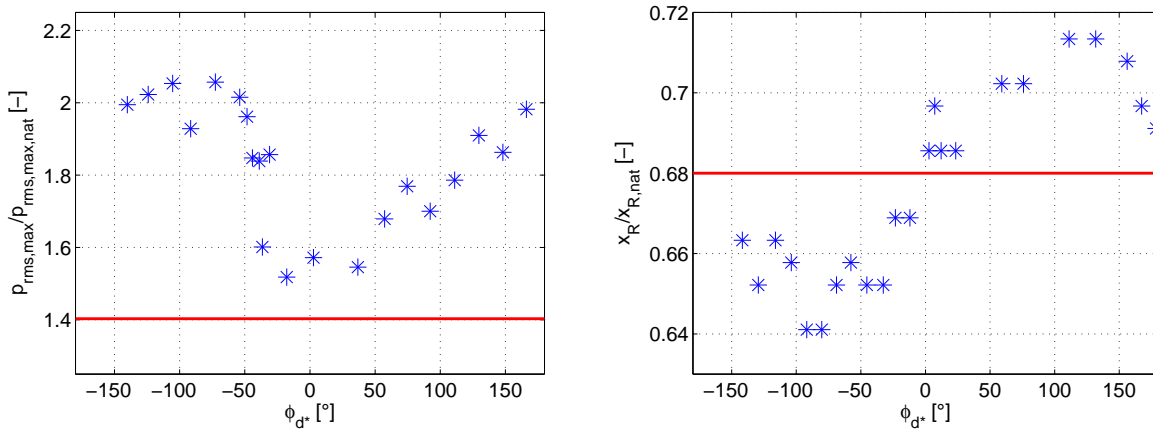


Figure 2. The flow over the backward facing step. Left: Maximum pressure fluctuations normalized by the level of the natural flow for the flow under open- and closed-loop actuation. Right: Comparison of the period average of the reattachment point x_R , normalized by the reattachment length of the natural flow. The red lines refer to the open-loop actuation, the blue dots to closed-loop actuation.

III. A Phasor Model and an Observer for the Free Shear Layer

A. The free shear layer

The two dimensional free shear layer is an idealization of systems such as the wake behind a thin airfoil, where no boundary interactions occur past the inception of the shear layer. A schematic is depicted at the top of Figure 3, featuring the discrepancy between the incoming flow velocities above and below a separating wall, and the growth of the of the shear layer as it evolves, downstream. Both Kelvin-Helmholtz vortices and vortex pairing are apparent in the shear layer visualization at the bottom plot of Figure 3. The flow velocity along the shear layer is the average of the two input velocities, and shear layer vortices convect at that velocity, creating a simple relation between the vortex generation frequency and the spatial wave length (i.e., the average distance between vortices in the near field). A natural instability determines a peak sensitivity at a characteristic frequency, but the flow is sensitive to disturbances at a range of frequencies, a fact that is reflected by seemingly random drifts in the upstream periodic behavior as well as aperiodic vortex pairing, further downstream.

For rapid prototyping and observer proof of concept we use a moderate order simulation vortex model. Its main parameters are: Incoming flow velocities of $U_1 = 1.5$, $U_2 = 0.5$, hence a shear layer velocity of $U_s = 0.5(U_1 + U_2) = 1$. The initial vortex core radius, defining the characteristic length, is $R = 1$

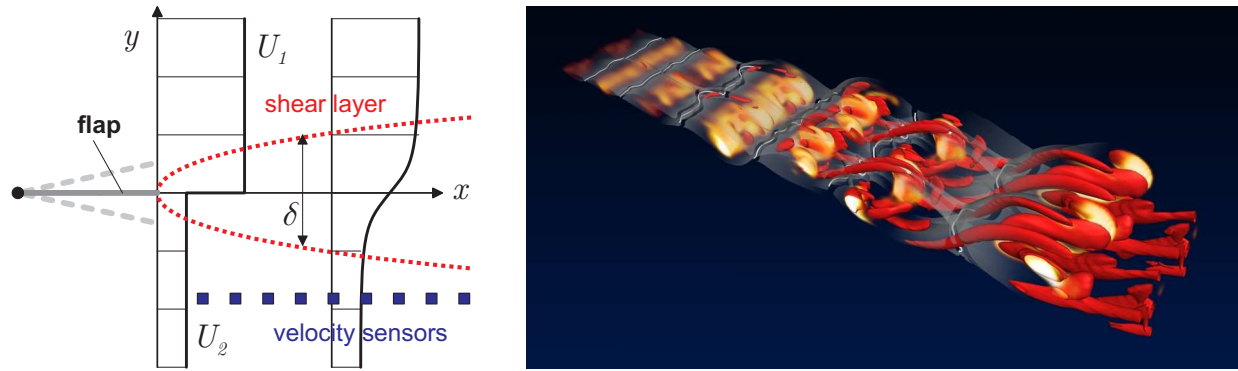


Figure 3. Left: A schematic of the free shear layer with a flap actuator and velocity sensors located below the shear layer. Right: Visualization of a detailed 3D numerical simulation from Ref.³³ using the source term Q of the pressure-Poisson equation. The primary Kelvin-Helmholtz vortices in the early shear layer are marked by a yellow volumetric representation of $Q \cos^2 \theta < 0$, where θ is the local angle between the vorticity vector and the spanwise direction. Rib vortices in the later shear layer are represented by red iso-surfaces of $Q \sin^2 \theta$.

and the circulation production rate is $dG/dt = -1$. The Strouhal number (i.e., the natural instability frequency, normalized by the characteristic length and period) is $St = fR/U = 0.05$, leading to a frequency of $\omega = 0.1\pi$, time period $T = 20$ and spatial wave length $\lambda = 20$. Periodic actuation at the instability frequency is represented by an oscillating flap at the end of the separating wall (Figure 3, top). The flap length is $\lambda = 20$ and the vertical oscillation stroke is 0.05λ .

Random perturbations and drift in the periodic behavior will be a challenge in observer design, where the objective is the estimation of the center location of vortical structures from data obtained from an array of sensors. As will be seen in the backward step benchmark, this information can be used to further harmonize vortex release, enhance shear layer growth and increase its mixing effect. Locating vortex position can also be used in a control aiming to enhance or delay vortex merging by local actuation at a specific location along the shear layer.^{13,19,31} Here we shall only discuss the dynamic estimation component. In that context we postulate measurements of the stream-wise fluid velocity at 24 points along the line $y = -15$ (relative to Figure 3). Velocity sensors were selected due to the relative ease to incorporate them in the vortex model we use to test the suggested framework, but the proposed estimation framework is equally applicable to more practical alternatives, such as pressure gages, as is done in the experimental setup used in our next benchmark, in §A.

B. A Free Shear Layer Observer

Here we highlight features added to the previous case, to address the presence of asynchronous vortex merging. The sampled trajectory of velocity measurements is denoted $\mathbf{u}_m(t) = (u_m(t, (x_i, -15)))_i$, and the observer estimates the x -coordinates of shear layer vortices.

The Near Field Shear Layer ($0 \leq x \leq 4\lambda$):

Vortices do not merge and maintain the time frequency ω , the spatial wave length λ , and a convection velocity of U_s .

- The $[0, 4\lambda]$ component of \mathbf{u}_m forms a single harmonic traveling wave. Its spatio-temporal Fourier coefficients are ideally constants. Dynamic corrections are obtained by the low pass filtered deviation between the coefficients of the projected instantaneous wave form and previous estimates. The used filter time constant is $0.67T$.
- Stream-wise velocity below the shear layer is negative. Local minima indicate passing vortices. Measured locations of local minima are easily extracted from the reconstructed single (first) harmonic wave form.
- As a vortex estimate reaches $x = 4\lambda$, it is handed over to the downstream observer and a new upstream vortex location is estimated at $x = 0$.

The Downstream Shear Layer ($4\lambda \leq x \leq 14\lambda$):

Estimation of individual vortex locations becomes local and the convection velocity varies between vortices due to the effect of paired vortices and varying distances between them. The dynamic estimates for each vortex therefore includes *both* the position \hat{x}_i and convection velocity \hat{u}_i , initiated at 4λ and U_s , respectively. Measured corrections, as described below, are low pass filtered with a long time constant.

- A vortex pair is merged and the estimator for one of the two is removed once their estimated horizontal distance reduces below a tolerance $\eta = 2 = 0.1\lambda$.
- We distinguish between several cases, relating to the position and convection velocity of the i^{th} vortex:
 - If the $i + 1^{st}$ vortex is a merged (double) vortex, its effect on sensor readings is typically larger than that of the i^{th} vortex, excluding the search for- and use of the location of a local minimum in the measured fluid velocity below the i^{th} vortex. The $i + 1^{st}$ vortex has an accelerating effect on the i^{th} vortex. A very simple way to correct for that effect is as follows: At the time t_{k+1} , the sensor readings over the interval $[\hat{x}_i(t_k), \hat{x}_i(t_k) + 2\lambda]$ are projected over the 1^{st} spatial subharmonic. The located minimum of this waveform indicates a point \bar{x}_{i+1} of maximal effect of the merged vortex. This position is used as a low pass filtered update for the next position: $\hat{x}_i(t_{k+1}) = (1 - \nu)\hat{x}_i(t_k) + \nu\bar{x}_{i+1} + \hat{u}_i(t_k) \cdot \Delta t$, with the corresponding update on the convection velocity. A long filter time constant of $8T$ was used.
 - Else, the second harmonic expansion of sensor signals is evaluated over the interval $[\hat{x}_i(t_k) - 0.25\lambda, \hat{x}_i(t_k) + 0.25\lambda]$. If this expansion attains a minimum over $[\hat{x}_i(t_k) - 0.125\lambda, \hat{x}_i(t_k) + 0.125\lambda]$, that minimum will be used as a new measured position, and low pass filtered (with a time constant of $0.8T$) to update both $\hat{x}_i(t_{k+1})$ and $\hat{u}_i(t_{k+1})$. Sharper minima due to the presence of paired vortices motivates the use of the 2^{nd} harmonic.
 - Else, the first harmonic expansion of sensor signals is evaluated over the interval $[\hat{x}_i(t_k) - 0.5\lambda, \hat{x}_i(t_k) + 0.5\lambda]$. If this expansion attains a minimum over $[\hat{x}_i(t_k) - 0.25\lambda, \hat{x}_i(t_k) + 0.25\lambda]$, it will be used as a measured position in updates, as above.
 - If no local minimum is found, no velocity update is applied: $\hat{u}_i(t_{k+1}) = \hat{u}_i(t_k)$ and $\hat{x}_i(t_{k+1}) = \hat{x}_i(t_k) + \hat{u}_i(t_{k+1}) \cdot \Delta t$.

Figure 4 depicts two generic snapshots of the vorticity distribution in the flow and dynamic estimates of the locations of vortical structures. The figure illustrates both near field shear layer vortex tracking and a reasonable ability to continue tracking vortices as they aggregate into larger structures. Some local estimation distortions are due to the effect of variations in the vertical vortex positions on the measured velocity. These variations are not accounted for in the simple model used here, illustrating the potential advantages of including more details, such as using a Biot-Savart equation in the context of aggregated vortices, as a forward model in a dynamic inverse problem solution.

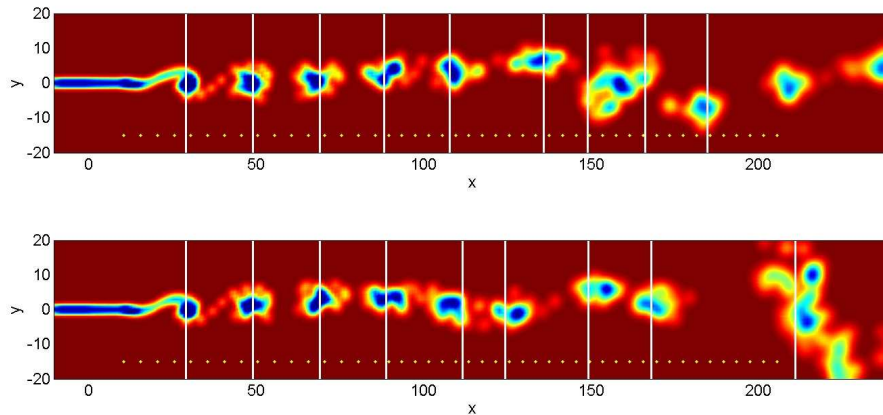


Figure 4. Snapshots of the vorticity distribution and vortical structures tracking in the free shear layer. Dark spots indicate high vorticity. Vertical lines are estimates of vortex location and yellow dots along $y = -15$ indicate velocity sensors. Estimates downstream of the last sensor are not updated.

IV. Concluding Remarks

A proposed simple observer structure estimates vortex locations along a shear layer from an array of velocity or pressure sensors. It is based on a phenomenological dynamic phasor model for the traveling waveform of sensors' readings. The dynamic estimate provides phase information that enables harmonic corrections in a periodic actuation signal, in order to manipulate and increase shear layer growth, with beneficial effects on mixing. The observer is illustrated in both simulations and closed loop control experiments for the flow over a backward facing step, and in a free shear layer simulation. Future works may include means to enhance the tracking capability of the observers under closed-loop actuation. Another question is, whether the used scheme to determine the reattachment length by evaluating the position of the maximum pressure fluctuations is meaningful under closed-loop actuation or not. The effect of closed-loop actuation on pressure recovery is under current investigation.

Acknowledgments

We acknowledge funding of the Deutsche Forschungsgemeinschaft (DFG) and the U.S. National Science Foundation (NSF). DFG support was via the Collaborative Research Center (Sfb 557) "Control of complex turbulent shear flows" at the Berlin University of Technology and by the grants NO 258/1-1 and DI 448/5-1. NSF support was via grants No. 0136404, 0410246 and 0230489.

We thank Tino Weinkauff and his team for stimulating discussions and revealing feature extractions. The 3D visualizations have been prepared with Amira (ZIB).

References

- ¹A. MICHALKE. On spatially growing disturbances in an inviscid shear layer. *J. Fluid Mech.* **23**, 521 – 544, 1965.
- ²P.G. DRAZIN & W.H. REID. *Hydrodynamic Stability*. Cambridge University Press, 1981.
- ³R. R. RUDERICH & H.H. FERNHOLZ. An experimental investigation of a turbulent shear flow with separation, reverse flow and reattachment. *J. Fluid Mech.* **163**, 283–322, 1985.
- ⁴B. COLLIER, B. R. NOACK, S. NARAYANAN, A. BANASZUK & A. I. KHIBNIK. Reduced basis model for active separation control in a planar diffuser flow. *AIAA Paper* **2000-2562**.
- ⁵B.R. NOACK, I. MEZIĆ, G. TADMOR & A. BANASZUK. Optimal mixing in recirculation zones. *Phys. Fluids* **16**, 867–888, 2004.
- ⁶M.A.Z. HASAN. The flow over a backward-facing step under controlled perturbation: laminar separation. *J. Fluid Mech.* **238**, 73–96, 1992.
- ⁷T. R. BEWLEY. Flow control: new challenges for a new renaissance. *Progress in Aerospace Sciences* **37**, 21 – 58, 2001.
- ⁸M. GUNZBURGER. *Perspectives in Flow Control and Optimization*. SIAM, 2002.
- ⁹O. AAMO & M. KRSTIC. *Flow Control by Feedback Stabilization and Mixing*. Springer, 2003.
- ¹⁰R. M. MURRAY (ED.). *Control in an Information Rich World: Future Directions in Control, Dynamics, and Systems*. SIAM, 2003.
- ¹¹L. CATTAFESTA, D.R. WILLIAMS, C.W. ROWLEY & F. ALVI. Review of active control of flow-induced cavity resonance. *AIAA Paper* **2003-3567**.
- ¹²G. TADMOR. Control of a dual drive to attenuate switching frequency ripple in a large permanent magnet synchronous motor. *IEEE Trans. Control Systems Tech.*, 2003.
- ¹³G. TADMOR. Observers and feedback control for a rotating vortex pair. *IEEE Transactions on Control Systems Technology* **12**, 36 – 51, 2004.
- ¹⁴J. GERHARD, M. PASTOOR, R. KING, B.R. NOACK, A. DILLMANN, M. MORZYŃSKI & G. TADMOR. Model-based control of vortex shedding using low-dimensional Galerkin models. *AIAA Paper* **2003-4262**.
- ¹⁵B.R. NOACK, G. TADMOR & M. MORZYŃSKI. Low-dimensional models for feedback flow control. Part I: Empirical Galerkin models. *AIAA Paper* **2004-2408**.
- ¹⁶G. TADMOR, B.R. NOACK, M. MORZYŃSKI & S. SIEGEL. Low-dimensional models for feedback flow control. Part II: Controller design and dynamic estimation. *AIAA Paper* **2004-2409**.
- ¹⁷B.R. NOACK, K. AFANASIEV, M. MORZYŃSKI, G. TADMOR & F. THIELE. A hierarchy of low-dimensional models for the transient and post-transient cylinder wake. *J. Fluid Mech.* **497**, 335–363, 2003.
- ¹⁸Y.K. SUH. Periodic motion of a point vortex in a corner subject to a potential flow. *J. Phys. Soc. Jap.* **62**, 3441–3445, 1993.
- ¹⁹D. VAINCHTEIN & I. MEZIĆ. Control off a vortex pair using weak external flow. *J. of Turbulence* **3**, 51, 2002.
- ²⁰F. LI & N. AUBRY. Feedback control of flow past a cylinder via transverse motion. *Phys. Fluids* **15**, 2163–2176, 2003.
- ²¹M. PASTOOR, R. KING, B.R. NOACK, A. DILLMANN & G. TADMOR. Model-based coherent-structure control of turbulent shear flows using low-dimensional vortex models. *AIAA Paper* **2003-4261**.
- ²²B. PROTAS. Linear feedback stabilization of laminar vortex shedding based on a point vortex model. *Phys. Fluids* **16**, 4473–4488, 2004.

- ²³B.R. NOACK, P. PAPAS & P.A. MONKEWITZ. The need for a pressure-term representation in empirical Galerkin models of incompressible shear flows. *J. Fluid Mech.* **523**, 339–365, 2005.
- ²⁴C.L. DEMARCO & G.C. VERGHESE. Bringing phasor dynamics into the power system load flow. In *North American Power Symposium*, 463–469, 1993.
- ²⁵G. TADMOR. On approximate phasor models in dissipative, bilinear systems. *IEEE Transaction on Circuits & Systems I: Fundamental Theory*, **49**, 1167 – 1179, 2002.
- ²⁶G. TADMOR & A. BANASZUK. Observation feedback control of vortex motion in a recirculation region. *IEEE Transactions on Control Systems Technology* **10**, 749 – 755, 2002.
- ²⁷T. WEINKAUF, H.-C. HEGE, B.R. NOACK, M. SCHLEGEL & A. DILLMANN. Coherent structures in a transitional flow around a backward-facing step. *Phys. Fluids*, **15**, S3, 2003.
- ²⁸J. MABEY. Analysis and correlation of data on pressure fluctuations in seperated flow. *JoA* **9**, 642–645, 1972.
- ²⁹R. BECKER, M. GARWON & R. KING. Development of model-based sensors and their use for closed-loop control of separated shear flows. In *European Control Conference, University of Cambridge, UK*, 2003.
- ³⁰R. KING, R. BECKER, M. GARWON & L. HENNING. Robust and adaptive closed-loop control of separated shear flows. *AIAA Paper* **2004-2519**.
- ³¹T. SUZUKI, T. COLONIUS & D. G. MACMARTIN. Inverse technique for vortex imaging and its application to feedback flow control. *AIAA Paper* **2003-4260**.
- ³²T. SUZUKI & T. COLONIUS. Inverse-imaging method for detection of a vortex in a channel. *AIAA J.* **41**, 1743–1751, 2003.
- ³³T. WEINKAUF, B.R. NOACK, P. COMTE, A. DILLMANN AND H.-C. HEGE. Coherent-Structure Skeleton of a Turbulent Mixing Layer. Poster at the Gallery of Fluid Motion 2004. 57th Annual Meeting of the Division of Fluid Dynamics of the American Physical Society. See <http://vento.pi.tu-berlin.de/ts/noackbr/Weinkauf2004aps.PDF> for details.